Tuning separation behavior of tailor-made thin film poly(piperazine-amide) composite membranes for pesticides and salts from water

Romil Mehta [a], H. Brahmbhatt [b], M. Mukherjee [c], A. Bhattacharya [a,*]

[a] *Reverse Osmosis Division, CSIR-Central Salt and Marine Chemicals Research Institute (CSIR-CSMCRI), Council of Scientific & Industrial Research (CSIR), G. B. Marg, Bhavnagar 364002, Gujarat, India*
[b] *Analytical Division and Centralized Instrument Facility, CSIR-Central Salt and Marine Chemicals Research Institute (CSIR-CSMCRI), Council of Scientific & Industrial Research (CSIR), G. B. Marg, Bhavnagar 364002, Gujarat, India*
[c] *Saha Institute of Nuclear Physics, 1/AF Bidhannagar, Kolkata 700064, West Bengal, India*

HIGHLIGHTS

- Tailor-made thin film poly(piperizinamide) composite membrane.
- Membrane selectivity depends on the medium of interfacial polymerization.
- Partition co-efficient of piperazine in different medium supports the selectivity of the membrane.
- pH dependence of separation behavior of salts.
- Separation behavior of pesticides depends on the nature of molecules and pH of the feed.

ARTICLE INFO

ABSTRACT

The present study describes some appealing results concerning the TFC membrane performances prepared by varying the solvents of piperizine (viz. water, acetonitrile and water-acetonitrile). The membrane selectivity of bivalent over mono-valent anions reduces from water > acetonitrile-water > acetonitrile (i.e. Memb-I > Memb-II > Memb-III). The partition co-efficient values support the trend. The retention order of salts is $Na_2SO_4 > MgSO_4 > MgCl_2 > CaCl_2 > NaCl$. pH dependence separation study shows different behaviors for NaCl, Na_2SO_4 and $MgSO_4$. Memb-I and II show minimum NaCl separation at pH 7 whereas in acidic and alkaline medium it is increasing trend, but Memb-III shows differences in alkaline pH. On the contrary Memb-I and II show improvement in retention with pH for Na_2SO_4 and $MgSO_4$, whereas Memb-III shows the fall in retention at alkaline pH. The separation performance of diuron and isoproturon follows order $R_{isoproturon}(90.95\%) > R_{diuron}(79.34\%)$ for Memb-II at pH 7. The separation performances follow the trend Memb-II > Memb-I > Memb-III. It reflects that acetonitrile-water mixture for piperizine optimizes maximum permeability as well as a charge of the membrane. The higher retention of isoproturon at alkaline pH is explained by higher molecular size and low polarity compared to diuron. The low separation trend of diuron at higher pH may be explained by relatively more polarity and low molecular size.

© 2016 Elsevier B.V. All rights reserved.

1. Introduction

The growing global need for water and waste water treatment has driven the widespread development of membrane filtration processes. The membrane is not new to the step of availability of fresh water. The enormous history of membranes and made to order different filtration set up. Fast forward to present era. From ever-evolving orders for desalination to waste water treatment, the membranes take the footsteps.

The potential ability of these membranes to remove pesticides is dictated by 'water reuse' strategy. Water contamination occurs generally occurs as a consequence of using herbicides in agricultural activities. Much advancement of technological efforts has been taking place in the agricultural world. The adverse effects on human health are serious concern. Since water is one of the vehicles to transport in the food chain, scientists and technologists have the target to purify water from it.

For the last few decades, scientists have explored simple methodologies to transform available polymers into materials with excellent properties and applications. In this regard 'Thin film composite' membrane is a milestone in separation science [1,2].

Thin film composite membranes are a class of macromolecular features formed by the interfacial polymerization on the asymmetric membrane support. The attractiveness of selected 'thin film composite membrane' system stems from several factors. The most important one is undoubtedly the chemical and thermal stabilities of these relative to other conventional polymers; the simple preparation and the possibility to prepare categories which have a range of appealing performances. Many significant developments have been taken place in the past few decades regarding the preparation of thin film composite membranes in the world. The beauty of this technique is that it occurs at low temperature and does not require a catalyst. There are two main controlling steps in this particular membrane formation viz. preparation of asymmetric polysulfone membranes, polyamide formation through interfacial polymerization. Research works have been carried out by varying conditions (viz. Varying different amine, pH of amine solution, coating conditions, mixing of additives, solvents of acid chloride) to prepare tailor made membranes [3–9]. Reports are also available in terms of addition of different solvents (viz. dimethyl formamide, dimethyl sulfoxide) to the aqueous amine system to modify the cross-linked structure of m-phenylne diamine and trimesoyl chloride [7,10, 11].

In our study, an interfacial polymerization reaction has been used to prepare poly(piperazine-amide) (polyamide) membrane formation on Polysulfone support. The interfacial polymerization in our study was performed on water/acetonitrile- hexane interface. The technique can synthesize and attach functional materials on to Polysulfone surfaces by the polymerization reaction between hydrophilic piperizine ($C_4N_2H_{12}$), a secondary amine and N-heterocyclic one and hydrophobic 1,3,5 trimesoyl chloride ($C_9H_3Cl_3O_3$), multifunctional monomer at water/acetonitrile-hexane interface. The unique feature of the poly(piperazine-amide) membrane membranes is that it can provide more free volume to the skin, poly(piperazine-amide) layer because of its low energy of its chair conformation [12]. Thus it can be suitable for organics separation.

With the aim of observing the effect of partition coefficient for the interfacial polymerization the experiment is carried out by adopting a single strategy. The diamine is interfacially polymerized to polyamide, by changing its solvent, i.e. water, acetonitrile and a mixture of acetonitrile/water. This paper investigates the use of acetonitrile in the interfacial polymerization of cross-linked polyamide. The separation profiles in terms of salt and organic markers are also descriptors for the membranes. The selectivity of bivalent over monovalent ratios is interesting for poly(piperazine-amide) membrane. It is our study to compare the separation performance study of all tailor-made membranes of bivalent salts over monovalent ones [13].\
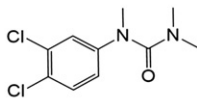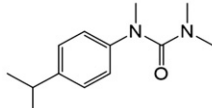
The aim of the present work was to study the removal of herbicides (viz. diuron, isoproturon) from aqueous solution by using different membranes prepared from changing its solvent, i.e. water, acetonitrile and a mixture of acetonitrile/water. The physical parameters are ensemble in Table 1 [14]. The separation of herbicides from aqueous solution is known to depend on the characteristics of membranes, feed solutes and the solution chemistry (i. e. pH). These factors were all taken to elucidate the process of herbicides separation through these membranes.

2. Experimental

2.1. Materials

Polysulfone Udel P-3500 was purchased from Solvay Advanced Polymers, USA. Piperizine (Across Organics, USA), trimesoyl chloride (Sigma, USA) were the prime chemicals used in thin film composite membrane preparation. N,N-dimethyl formamide (Loba, India), n-

Table 1
Properties of phenyl urea herbicides used in study.

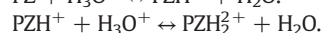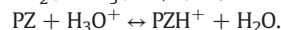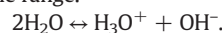| Diuron	Isoproturon
Molecular formula - $C_9H_{10}Cl_2N_2O$	Molecular formula - $C_{12}H_{18}N_2O$
Molecular weight, Da - 233.10	Molecular weight, Da - 206.9
Molecular size, nm - 0.781	Molecular size, nm - 0.810
Polarity (Debye) - 5.87	Polarity (Debye) - 3.31
Log k_{ow} - 2.78[13]	Log k_{ow} - 2.32[13]

hexane (Merck, India) was used as solvents. The non-woven polyester fabric was supplied by Filtration Sciences Corp., USA. Polyethylene oxide (PEO, 100 KDa, 200 KDa) (Sigma Aldrich, USA), Glucose and Sucrose (HIMEDIA Scientific, India) were used for the molecule markers of the membranes. Diuron, Isoproturon was supplied by Sigma- Aldrich, USA. Sodium chloride (Rankem, India), Sodium sulfate (Fisher Scientific, India), Magnesium sulfate (HPLC, India), Calcium chloride (FINAR Chemicals, India), Magnesium chloride (HIMEDIA Scientific, India) were used in the present study. Deionized water was used for all the experiments.

2.2. Preparation of asymmetric Polysulfone support

Polysulfone solutions (15% w/w) were prepared in hydrophilic aprotic solvent (N,N-dimethyl formamide) through slow heating and stirring condition. The high boiling point of N,N-dimethyl formamide has advantages as it needs heating during the preparation of polysulfone solution preparation. The solution was cast on the non-woven polyester fabric by a prototype casting machine (motor speed 2 m/min). The schematic diagram of the prototype casting machine is presented in Fig. 1. The fabric was first mounted on the roller (A) guided by roller attached to the speed control sensor (B). The casting blade (C) attached to micrometer (D) was adjusted to maintain the thickness of the polysulfone layer. After casting the polysulfone layered fabric was dipped into nonsolvent water (F) kept in to gelation bath) (E). It was rolled on to receiving roller (G) regulated by speed controlled device (H). The dehumidifier (I) was attached to polysulfone layer fabrication chamber. The immediate immersion of the cast one in to gelation bath (non solventwater) formed the solid phase and features the membrane (PS). The characteristic parameter of the membranes (MWCO (molecular weight Cut off) 100 KDa based on Polyethylene oxide (PEO) and pure water flux (PWF) 637.3 LMH at 0.14 MPa was determined.

2.3. Fabrication of polyamide thin film composite on asymmetric polysulfone support

The skin crosslinked polyamide layer was coated on polysulfone support by interfacial polymerization. The support layer was first dipped into the freshly prepared aqueous aliphatic diamine, piperizine, 2% (w/v) (pH 9.7) for 2 min. The aqueous solution of piperizine may be modulated as follows and this turns the pH of the solution is in the alkaline range.

$2H_2O \leftrightarrow H_3O^+ + OH^-$.
$PZ + H_3O^+ \leftrightarrow PZH^+ + H_2O$.
$PZH^+ + H_3O^+ \leftrightarrow PZH_2^{2+} + H_2O$.

Freshly prepared piperizine solution is preferred to avoid the reaction with carbon dioxide [15]. After decanting the piperizine solution the membrane was dipped into a hexane solution consisted of 0.1% (w/v) trimesoyl chloride for 2 min. The interfacial reaction of piperizine and trimesoyl chloride was occurred in water- hexane interface. The
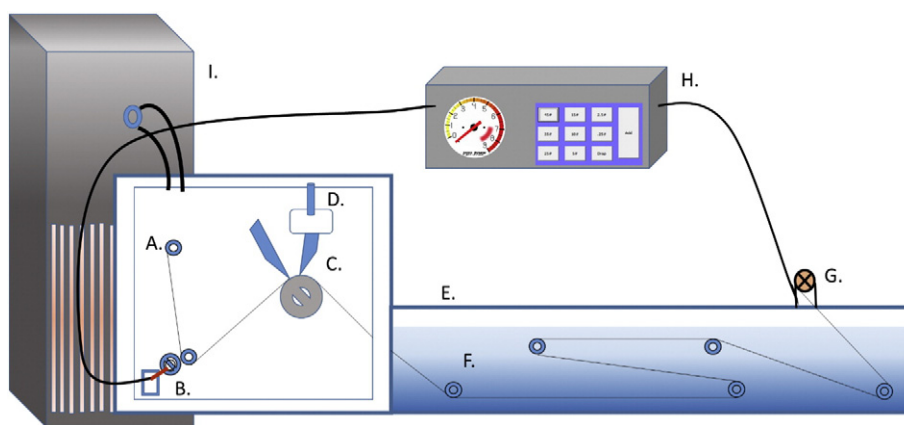
Fig. 1. Schematic diagram of proto-type casting machine for preparation of polysulfone support membrane. A. Mounting roll, B. Speed control sensor, C. Casting blade, D. Micrometer, E. Gelation bath, F. Non-solvent water, G. Receiving roller, H. Speed control device, I. Dehumidifier.

reaction is preferably at the hexane phase because of the low availability in aqueous phase similar to 1.3 phenylene diamine - trimesoyl chloride studied earlier [16]. The polyamide was cured at 100 °C for 4 min. The same reaction was also conducted using piperizine in acetonitrile-water (1:1) mixture and acetonitrile. The membrane is termed as Memb-I, Memb-II and Memb-III as in Table 2.

Thus three layer thin film composites were prepared. The schematic diagram is presented in Fig. 2. The top ultrathin layer is responsible for ion/molecule selectivity. Below the top ultrathin layer, the porous sub layer asymmetric in nature controls the feed flow as well as provided surface which accommodate polyamide thin layer. The macrovoid porous sublayer increases the mass transfer [17]. The third layer is a non-woven polyester fabric which holds the mechanical strength of the whole membrane.

2.4. Permeability studies

Permeation experiments were carried out by crossflow filtration technique at 1.034 MPa pressure. The cross-flow filtration setup is shown in our previous study [18]. Four pressure cells made of SS-316 are in a series. There was perforated support on which membrane was placed. TFC membrane was compacted 1 h before taking separation data. The effective membrane surface area in each cell was 0.00152 m^2. The salt (viz. NaCl, Na$_2$SO$_4$, MgSO$_4$, CaCl$_2$, and MgCl$_2$) concentrations were kept at 1000 mg/L. The molecular descriptors (viz. glucose, sucrose) were prepared (500 mg/L). The synthetic waste water was prepared with herbicides (viz. diuron, isoproturon) (2 mg/L). All the experiments are carried out in deionized water.

The permeate flux (J_v) was calculated by.

$$J_v = \frac{V}{A\,t}$$

where J_v is expressed in $lm^{-2}\,h^{-1}$, V (in litre) is the permeate volume, $A(m^{-2})$ is the membrane area and t (in hr) is the permeation time.

The separation (R%) is denoted by

$$R(\%) = \left(1 - \frac{C_p}{C_f}\right) \times 100$$

where C_p and C_f is the concentration (mg/L) of feed and permeate.

2.5. Analytical methods

The chemical structures of the membranes were analyzed by Fourier Transform Infrared Spectroscopy using attenuated total reflectance attachment (FTIR-ATR, Perkin Elmer Spectrum GX, Norwalk,CT with resolution of $\pm 4\,cm^{-1}$). The powder samples with KBr crystal (1:50) were taken for the measurements. The crosslinked polyamide powder samples were obtained by dipping crosslinked poly(piperazine-amide) membranes into NN dimethyl formamide. The polysulfone was dissolved in the solvent and poly(piperazine-amide) was separated out. The polyamide was then centrifuged and collected for the analysis. Contact angle of the membranes were carried out by sessile drop method (DSA 100, KRUSS, Germany) at 25 °C. The capture of water contact angle was 15 s. The zeta potential (ζ) was determined with the electrokinetic analyzer (Zeta-CAD, France (version 1.04) based on the streaming potential method using flat sheet's of the membrane material (5 × 3 cm) in a commercial plate taking 1 mM KCl as background electrolyte. X-ray diffractometer (PANalytical Empyrean), Cu K α radiation as monochromator was used to prove the changes the relative amorphous character for polyamide powders from the respective membranes. Scanning Electron Microscope (SEM) images of the samples were taken using JSM-7100 F. Atomic force microscopy (AFM) images of the samples were acquired using NT-MDT, Russia AFM instrument. XPS core-level spectra were taken with an Omicron Multiprobe (Omicron NanoTechnology GmbH, UK) spectrometer fitted with an EA125 hemispherical analyzer. A monochromated Al Kα X-ray source operated at 150 W was used for the experiments. The analyzer pass energy was kept fixed at 40 eV for all the scans. As the samples are insulating in nature, a low energy electron gun (SL1000, Omicron) with a large spot size was used to neutralize the samples. The potential of the electron gun

Table 2
Membrane preparation medium during interfacial polymerization and physical parameters.

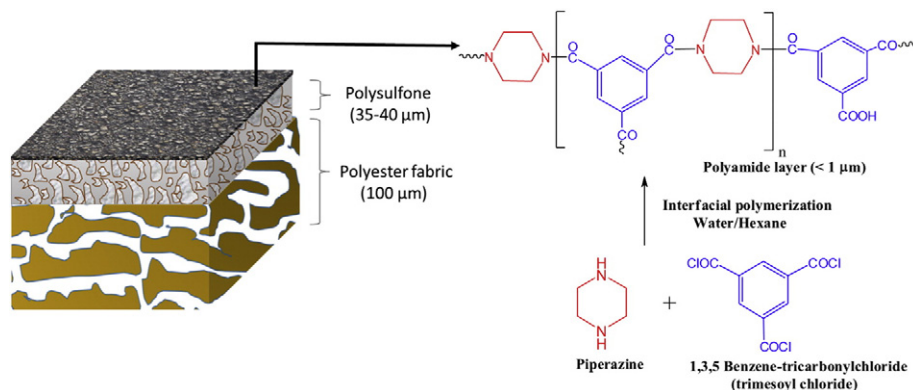| Membrane	Interfacial polymerization medium	Contact angle (θ°)		Surface roughness, Sa
		L	R	
PS	–	75.12 ± 1.77	76.48 ± 1.99	0.00508
Memb I	Water/hexane	32.35 ± 3.01	33.55 ± 1.52	0.0123
Memb II	Water:acetonitrile (1:1)/hexane	24.6 ± 2.58	26.64 ± 1.95	0.0139
Memb III	Acetonitrile/hexane	–	–	0.0233

Fig. 2. Schematic representation of thin film composite (TFC) and interfacial polymerization between piperazine and trimesoyl chloride.
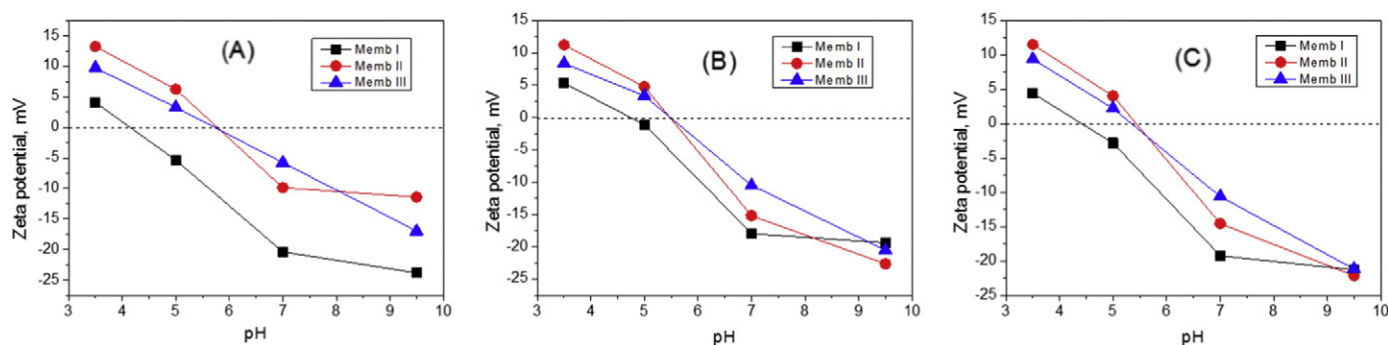

Fig. 3. Variation of Zeta potential of membranes with pH. A. background electrolyte KCl (1 mM), B. background electrolyte KCl (1 mM) + Na₂SO₄ (1 mM), C. background electrolyte KCl (1 mM) + MgSO₄ (1 mM).

was kept fixed at −3 eV for all the samples with respect to the ground. The binding energy of the peaks was corrected by considering the C1s peak of C——C bond to 284.8 eV.

The salt separations were calculated from their respective conductivities, as it exhibits a linear relationship with concentration. The conductivities of salts were determined by a conductivity meter. The concentration of organics (viz. glucose, sucrose, diuron, isoproturon)

Fig. 4. FTIR-ATR spectra of Polysulfone and Polyamide powders from their respective membranes.

were determined by High Performance Liquid Chromatography (Shimadzu Prominence model coupled with fluorescence detector) studies. The conditions employed for the estimation viz. C18H (enable) 150 mm × 4.6 mm × 5 μm, mobile phase acetonitrile/water (Rankem 80: 20) (containing 0.3% acetic acid, flow 1.0 mL/min, temperature 30 °C, injection volume: 50 μL)

The concentrations of glucose and sucrose were determined by Gel Permeation Chromatography (HPLC-GPC, Water Alliance-2695 separation module, with waters 2414RI detector) following the conditions column-supelco gel 610H, mobile phase 0.1% H_2SO_4 in water, flow 0.5 mL/min, temperature 30 °C, injection volume: 60 μL. The concentrations of macromolecule Polyethylene oxide (PEO 100KDa) were determined by Gel Permeation Chromatography (HPLC-GPC, water Alliance-2695 separation module, with waters 2414RI detector) following the conditions column-ultrahydrogel 120, mobile phase 0.2 mol of $NaNO_3$ in water, flow 0.8 ml/min, temperature 30 °C, injection volume: 60 μL.

Hydrophobicity is the simple manifestation of the relative insolubility of solutes in polar (i.e. water) and n-octanol (organic) medium. The simple mathematical form of the ratio of concentrations is termed as Partition co-efficient and designated as log P is expressed as log P = log (C_o/C_w) is termed as partition co-efficient. It is obvious the solute should be in the same molecular form where no association or dissociation occurs. In our present system piperizine is one of the key solutes in interfacial polymerization. The concentrations of piperizine in octanol- water medium were experimented with Total organic carbon analysis using TOC (Elementar, Germany). The experiment was extended to our system, i.e. piperizine in water-hexane as well as acetonitrile-hexane medium was as follows.

Piperizine (2% w/v) was taken in water-hexane (1: 1) as well as different water-acetonitrile-hexane mixture (Total volume 200 ml) in
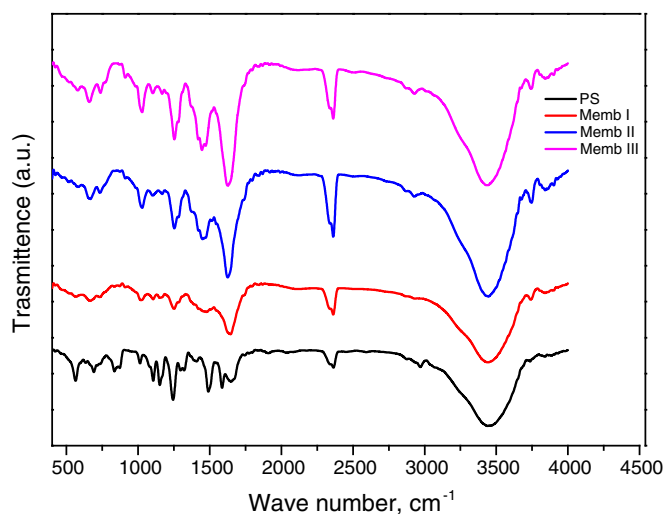
Table 3
XPS study of polyamide (from piperazine and trimesoyl chloride) and crosslinked (m) and linear (n) composition therefrom.

	C%	O%	N%	N/O (experimental)	N/O (theoretical)	m	n
Memb I	69	17	14	0.823	$\frac{(3m+2n)}{3m+4n}$	0.7087	0.2913
Memb II	70	17	13	0.765		0.6014	0.3995
Memb III	69	16	15	0.937		0.9029	0.0970

500 ml different sealed bottles. The bottle was shaken for 3 h at 100 rpm and settled for 15 min. The medium was separated and total organics analyzed in aqueous systems.

3. Results and discussion

In our experiment of wet phase separation process N,N-dimethyl formamide-water and polysulfone-N,N-dimethyl formamide dimixing in polysulfone/N,N-dimethyl formamide/water plays the key role in thin skin layer formation supported by porous structure. The phase separation occurs due to lowering of Gibbs free energy mixing because of the diffusion exchange of N,N-dimethyl formamide (solvent) and water (nonsolvent) across the interface of the casting solution [19–21].

The interfacial polymerization occurs on the asymmetric polysulfone support. The adsorption of diamine from its solution is because of the affinity of polysulfone towards diamine. This may be polarity due to the presence of —SO$_2$— in the unit of the polymer apart from the porous structure. The interfacial polymerization of piperizine occurs with trimesoyl chloride in hexane on the membrane support.

The aliphatic cyclic diamine having two dissociation constant (pk$_1$ and pk$_2$ 5.3 and 9.7) [22] when dissolved in water shows one is in ionic form and it slowly reacts with TMC to result polyamide. But in case of acetonitrile- water and acetonitrile medium there is less probability to ionize it because of low dielectric constant [23]. In the interfacial polymerization reaction the movement towards the hydrophobic hexane system is relatively more compared to the aqueous system. The partition co-efficient values also support that.

In our present system piperizine is one of the key solutes in interfacial polymerization. The concentrations of piperizine in octanol- water medium results −1.078 and verified with literature values (−1.17) [24]. The experiment was extended to our system, i.e. piperizine in water-hexane as well as acetonitrile- hexane medium. The variation shows that with the addition of acetonitrile the partition co-efficient increases and in acetonitrile-hexane mixture it is positive i.e. the trend of mixing of piperizine in hexane system is quite spontaneous. The partition co-efficient of piperizine in acetonitrile-hexane is higher (0.431) compared to water (−0.765) as well as water-acetonitrile (1:3) (0.174) and water-acetonitrile (1:1) (−0.144) system. Thus the solvent of aliphatic amine affects interfacial polymerization. The partition co-efficient of piperizine in acetonitrile-hexane couldn't change the side of reaction, probably because of preference of trimesoyl chloride presence in hexane, nonpolar one. The faster movement of piperizine (in

acetonitrile) towards the hexane i.e. trimesoyl chloride makes the polyamide low charge compared to polyamide prepared from water- hexane system. The zeta potential data for the membranes (Fig. 3) support the observation. Fig. 3 shows that Memb-II and III are the same of pHpzcs where as Memb-I showing slightly different. It may be because of variation of amino group present in the membrane.

FTIR analysis (Fig. 4) was performed to determine the functional group composition of polysulfone and polyamide powder samples as described above. The main characteristic absorption band (1152-1160 cm^{-1}) comes from —SO$_2$— of sulfone groups, frequently split into band groups. 1385–1365 cm^{-1} of spectrum is the signature of gem dimethyl groups of the matrix [25–27]. The specific bands 3200-3750 cm^{-1} appear for O—H stretching absorption is very strong and broad because of the presence of moisture, 1500–1600 cm^{-1} is due to the phenyl nucleus. The 1600 cm^{-1} band appears as phenyl is conjugated with groups having lone pair of electrons. 1250 cm^{-1} and 1320 cm^{-1} stretching mode (—C—O—C—) are present in the spectrum.

In case of piperizine-trimesoyl chloride based polyamide, the crosslinking product amide (—CON<) 1630 cm^{-1} is due to carboxylic acid and amide. 1450 cm^{-1} is for >CH$_2$ in polyamide layer. 1725–1600 cm^{-1} (>C═O) presence of carboxylic acid. It is seen that with the percentage increase of acetonitrile solvent in interfacial polymerization, the peak intensity for the >C═O regions (1630 cm^{-1}) is increased. It may be due to high partition co-efficient of piperizine (in acetonitrile - hexane) the polyamide formation is more facile and it is reflected from the weight difference of the membranes, which reflects from the order in terms of weight Memb-III (124.42 g/m^2) > Memb-II(120.97 g/m^2) ≥ Memb-I(120.12 g/m^2). It indicates that Memb-III has quite difference in weight where as Memb-II and Memb-I shows marginal difference or may be no difference at all. The data is the average of six pieces of membrane samples, having area 18.84 cm^2. The interesting point to note the variation of amide stretching in the spectrum of Memb-I to Memb-III. In water–hexane system the amide vibration is minimum due to relatively slow kinetics because of high partition co-efficient of piperizine whereas in the system of acetonitrile-hexane system the amide vibration is prominent due to relatively faster kinetics because of low partition co-efficient of piperizine (−0.765). Prominency of –N < in the crosslinked polyamide in acetonitrile-hexane system lowers the negative charge in the membrane as the zeta potential sequence suggests (Fig. 3). On the other hand the lower intensity of —N< in the crosslinked polyamide in water-hexane system generates higher –ve charge because of the facile formation of —COOH group in the system.

Similar observation is reflected in XPS study. The chemical composition obtained through XPS derived from the top polyamide layer. Table 3 ensembles the concentration percentages of C$_{1S}$, O$_{1S}$ and N$_{1S}$ of the different membranes. However Memb-II does not fit with the trend because of the small differences. It is more towards the results of Memb-I.

Considering the possibilities of two structure(s) i.e. cross-linked and linear (Fig. 5) the N/O value is the determining factor [28,29]. Considering m + n = 1, it is seen m has higher for Memb-III compared to Memb-I. It indicates that the cross linked structure is more for Memb-III to Memb-I, which is reflected in FTIR-ATR studies. The linear structure percentages in decreasing from Memb-I to Memb-III, reflect the ionic character supported by Zeta potential study as well as a bivalent-monovalent separation difference.

Fig. 6 shows the surface morphological pattern of different composite membranes. There are differences between three composite
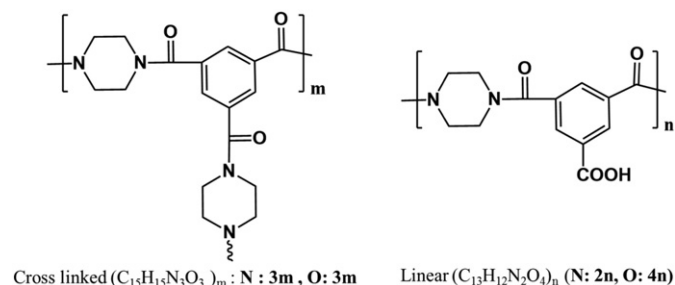

Cross linked $(C_{15}H_{15}N_3O_3)_m$: N : 3m , O: 3m   Linear $(C_{13}H_{12}N_2O_4)_n$ (N: 2n, O: 4n)

Fig. 5. Structure of polyamide (crosslinked and linear) from piperazine and trimesoyl chloride.
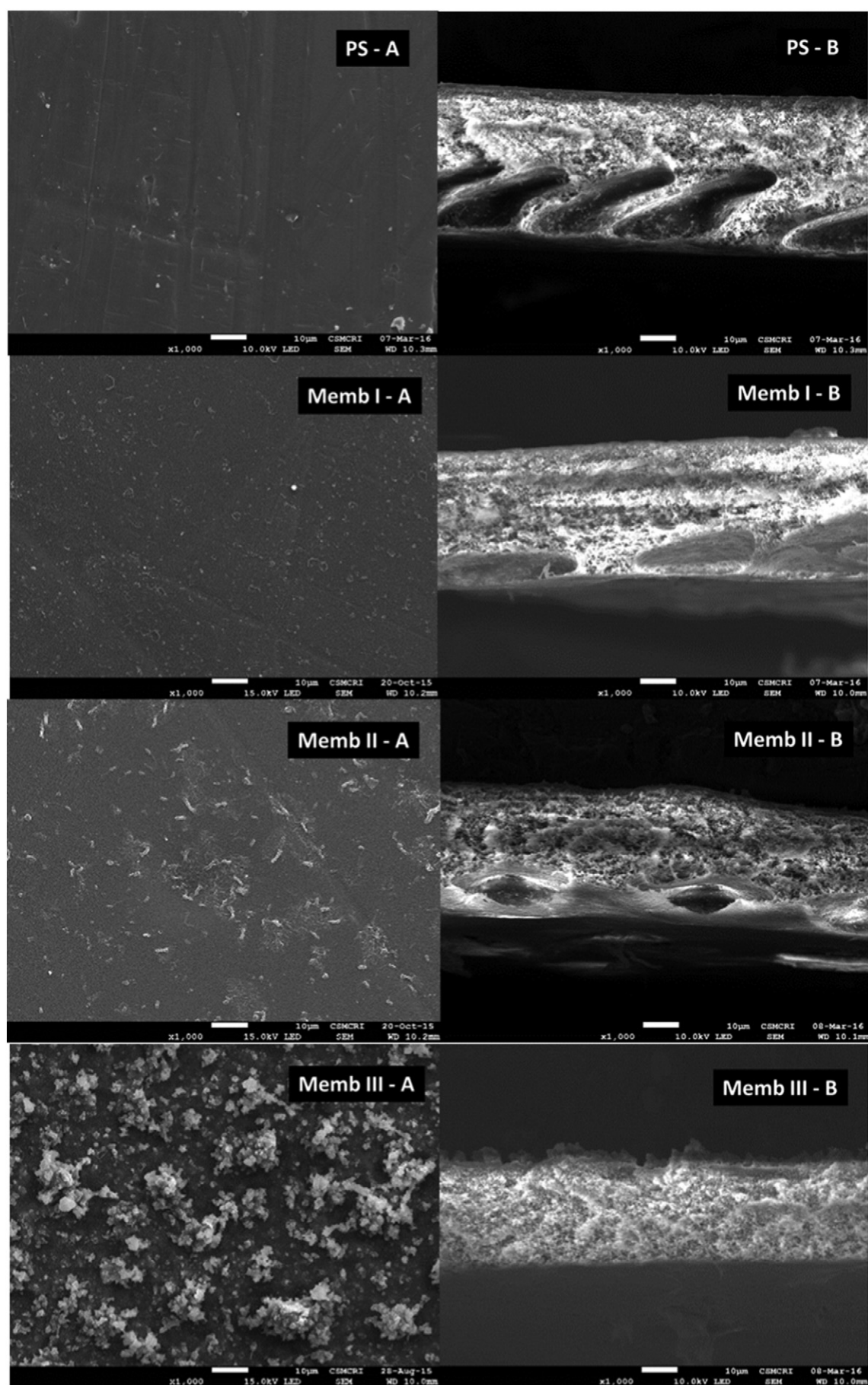
Fig. 6. Scanning electron microscopic images. A. top surface view and B. cross section view of polysulfone and TFC membranes.
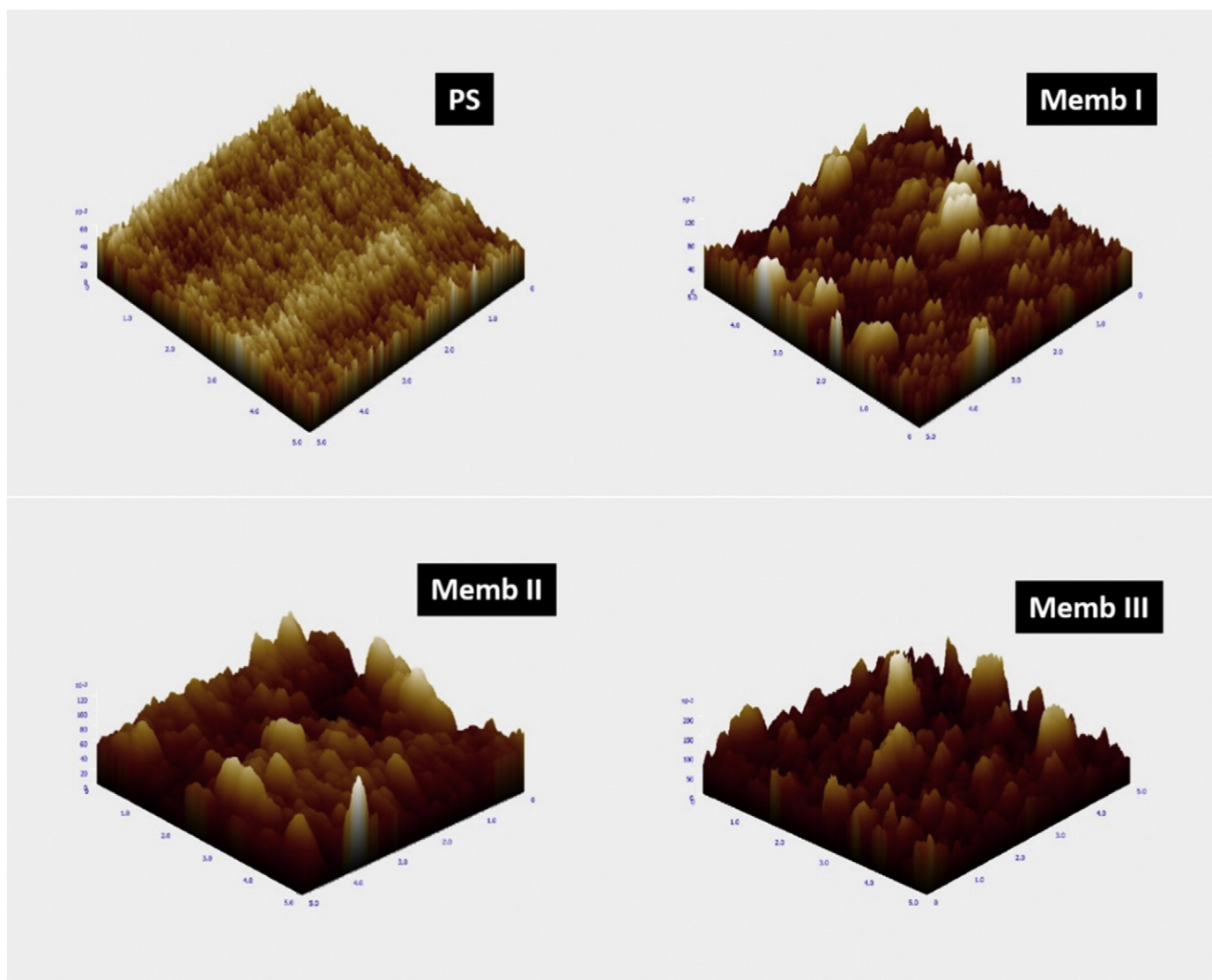
Fig. 7. AFM images of polysulfone and TFC membranes.

membranes (Memb-I, II and III) as well as virgin asymmetric Polysulfone membranes (PS), which is quite smooth. The polyamide shows like to disperse particles over the surface from Memb-I to Memb-III. The behavior is prominent from Memb-I to Mem-III. Moreover, the dispersed particles are in accumulated form in Memb-III. The cross-section view is also interesting. The asymmetric structure is well reflected in Polysulfone (B). The asymmetric structure is rather compressed from Memb-I to Memb-III. The growth of nodular shaped on the surface is seen in the Mem-III. These results are consistent in roughness parameters from Atomic Force Micrograph (Table 1). The micrographs are in the ensemble (Fig. 7). There is quite an appreciable difference in roughness between Memb-I and Memb-III.

Fig. 8 shows that Polysulfone is amorphous in character and presents one wide, weak broad peak at around 18° and similar to report by Ionita et al. [30].

The polyamides prepared from piperizine and trimesoyl chloride shows less amorphous character compared to polysulfone. The pattern is the signature of the amorphous character of polyamides. Though there is not prominent difference, the relative amorphous character of polyamide powder is Memb-I > Memb-II > Memb-III.

Contact angle studies (Table 2) show that Polysulfone membrane is hydrophobic. The polyamide coating on the polysulfone membrane makes them hydrophilic. The hydrophilicity trend is Memb-

III > Memb-II > Memb-I. The contact angle of Memb-III is not measurable. It shows spreading of water droplets over the membrane surface.

3.1. Separation of electrolytes

The performance of salt separation depends on the charge bears with membrane. The separation of electrolytes is discussed through different models [31]. The selectivity of bivalent over monovalent salts for poly(piperazine-amide) thin film composite membrane is already reported and explained in our report by density functional theory experiment [2,13,32].

The most promising model concept is based on Nernst Planck Equation, in which the total separation of electrolytes contribution attributed to electrical, diffusion and convection forces.

It is understood that when electrolyte is in contact with –vely charged membrane, the counter ions are in the vicinity of the membrane which forms the Donnan potential between the concentration difference of ions at the boundary between the membrane and bulk solution. Because of the Donnan potential the counter ions is attracted towards the membrane where as co-ions rejection takes place. Higher Donnan potential reflects higher salt rejection of the membrane [33,34].

The separation contribution comes from the hindrance of membranes to diffuse the ionic solute and solvent through it. In case of
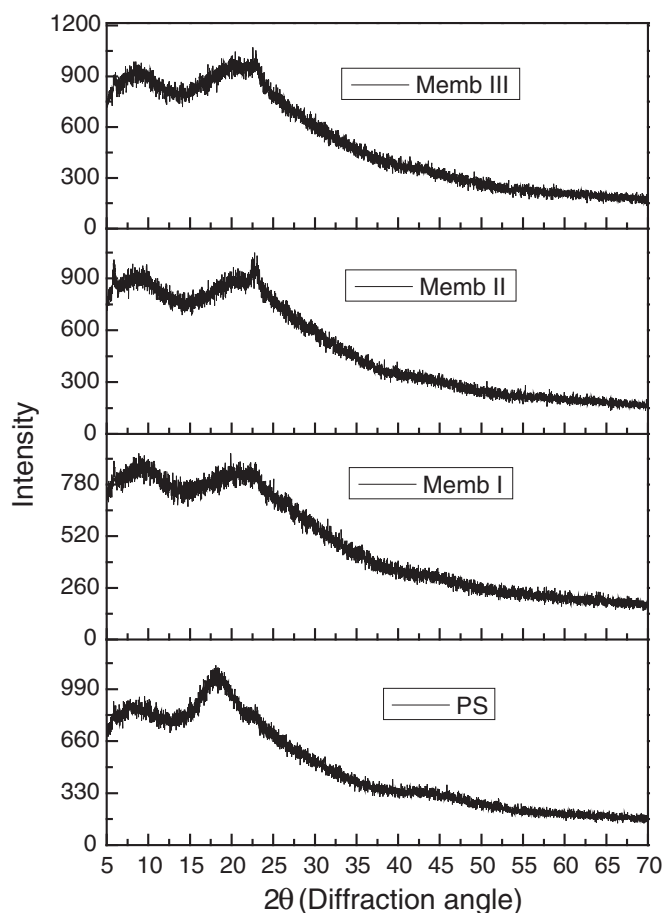
Fig. 8. X-ray diffraction pattern of polysulfone and polyamide powders from their respective membranes.

pore dimensions are of similar order to that of the solute molecule, the apparent diffusion co-efficient of the solute is much lower than that in bulk solution [31,35] whereas the convective hindrance to flow through it depends on the ionic radius and pore size.

The separations of different electrolytes are also in ensemble (Fig. 9 and Table 4). The charge, lower diffusion co-efficient, higher size ($SO_4^=$ 1.06×10^{-9} m^2/s, 0.23 nm) (Cl$^-$ 2.01×10^{-9} m^2/s, 0.12 nm) play role in case of Na$_2$SO$_4$ > NaCl and MgSO$_4$ > MgCl$_2$ separation. The higher diffusivity and lower size facilitates the permeation of Na$^+$ and thus the
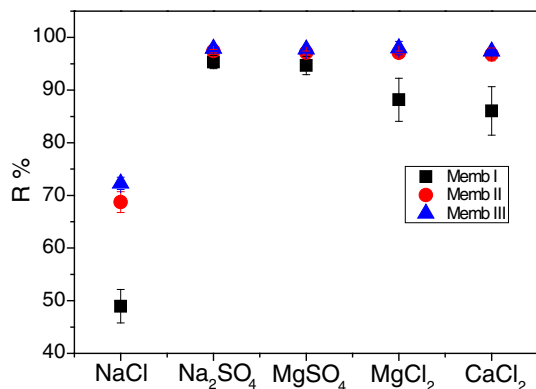

Fig. 9. Separation of salts of three TFC membranes.

rejection of NaCl is lowest. On the other hand low diffusivity and higher size of Mg^{2+} added the contribution of rejection of MgCl$_2$ and thus the ratio of Na$_2$SO$_4$/NaCl is higher than MgSO$_4$/MgCl$_2$ [34,36–38]. The hydrated size factor of the cations also plays the role in case of MgCl$_2$ > CaCl$_2$. It is well understood that the high retention of salts (bivalent co-ion + monovalent counter ion) and the lower retention of salts (bivalent counter ion + monovalent co-ion) from the Donnan exclusion model. The order of rejection of all the studied salts is Na$_2$SO$_4$ > MgSO$_4$ > MgCl$_2$ > CaCl$_2$ > NaCl. The same trend was observed for different commercial membranes reported by researchers [36,39]. The adsorption of Mg^{2+} on the membrane lowers the zeta potential of the membrane and thus the order suggests MgCl$_2$ > NaCl. Similar behavior was also seen in literature [16,37,39,40]. The diffusivity and size factor supports the order. (D$_{MgCl2}$: 1.24×10^{-9} m^2/s $<$ D$_{NaCl}$: 1.6×10^{-9} m^2/s) and (r$_{s\,(Mg}^{2+)}$ 0.35 nm $>$ r$_{s\,(Na}^{+)}$ 0.18 nm). All the rejection trend of salts is similar to all the three membranes. The selectivity of bivalent to monovalent salts (SO$_4^=$/Cl$^-$) decreases from Membrane I (1.95) to Membrane III (1.35). It can correlate with the decrease in zeta potential of the membranes. With the acetonitrile system, it diminishes the selectivity ratio as well as flux compared to aqueous one.

Regarding cationic separation of membranes, the cations with low diffusivities and higher pore size have the better rejection. In this regard the general retention order is Mg^{2+} > Ca^{2+} > Na$^+$. The Mg^{2+} (in MgSO$_4$) has better permeation than Mg^{2+} (in MgCl$_2$). Na$^+$ (in Na$_2$SO$_4$) has better permeation than Na$^+$ (in NaCl). In the –vely charged nanofiltration membrane the repulsive force acts on the co-ions (anion) and attractive force acts on counter-ions (cations). Divalent anion (SO$_4^=$) shows the higher charge effect compared to monovalent anion (Cl$^-$) and they are unable to pass through the membrane. But the oppositely charged divalent counter ions have no difficulty in passing through the membrane.

The zeta potential (ζ) varies with pH (Fig. 3). The pH dependence of the zeta potential gives information on the acidic and basic strength of the surface charge groups. In the alkaline range it shows negative plateu for the membranes I, II and III. This is due to the dissociation of acidic (−COOH) surface groups. The repulsive force between the –ve charge and the co-ion results higher rejection. At acidic pH (pH 3.5), the amino group being protonated and generates a positive charge on the membrane as the zeta potential suggests. The repulsive force between the Na$^+$ and membrane shows the higher rejection compared to neutral pH. This trend is same for Memb-I and Memb-II. Though the charged membranes repel co-ions (i.e. same sign of charge as the membrane charge) by the electric repulsive force, the cations couldn't be in the feed side independently, it will be there maintaining electro neutrality.

Fig. 10 show the performance variation with pH. In case of Na$_2$SO$_4$, the pH effect is same for Memb-I and Memb-II in the alkaline range as NaCl. Only the extent is small, as the retention has already reached 95% at normal pH. In acidic condition, the pH effect shows opposite with respect to NaCl rejection. It may be a higher anionic charge possessed by SO$_4^=$. Thus the repulsive force between membrane and SO$_4^=$ operates unlike in NaCl. The same trend is observed for MgSO$_4$ for the two membranes Memb-I and Memb-II.

But for Memb-III the opposite effect is observed in the alkaline pH region in all three salts (NaCl, Na$_2$SO$_4$, MgSO$_4$). The lower rejection of co-ion may be due to the excess counter-ion (viz. Na$^+$, Mg^{2+}) in the vicinity of the membrane which may lower the negative charge on it. At alkaline pH, OH$^-$ retention is much more (salt rejection is less). Thus the H + concentration in the permeate is much more and pH will be less. The pH changed to 8.5 from feed pH 9.51 for NaCl. The variation is not so much prominent with respect to three membranes. The reflection is a little bit more in case of other two salts (viz. 8.3 from pH 9.51 for Na$_2$SO$_4$ and MgSO$_4$).

In acidic condition nitrogen being protonated on the membrane, there is the possibility of electrostatic repulsion between the positive charge on the membrane and H$^+$ in the feed and results shrinkage of pores. Results showed that there is no significant variation in flux. In
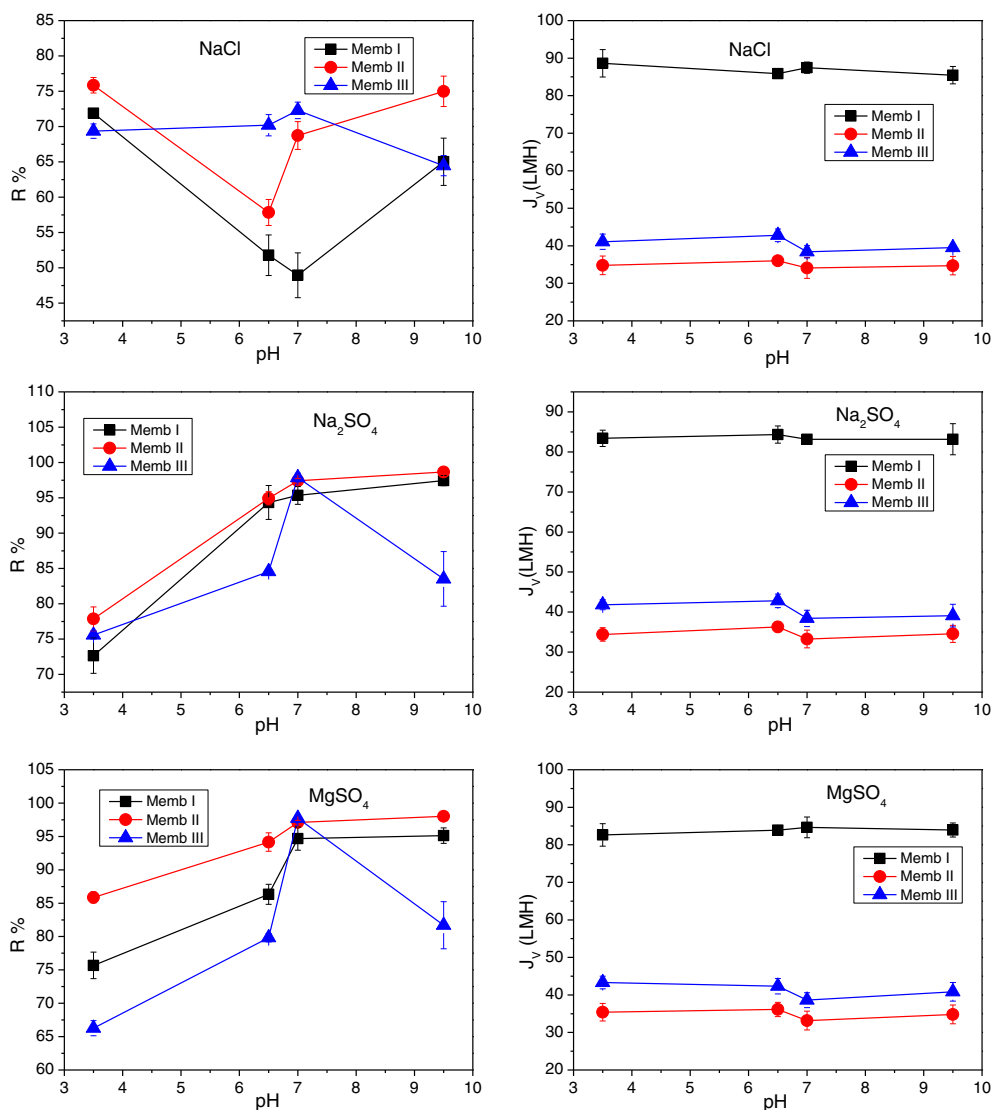
Fig. 10. Variation of rejection performances of salts with pH.

acidic pH, the protonated amino group takes the initiative. It repels H$^+$ in the feed. Thus permeate pH will be enhanced (3.51 to 5.95 for NaCl in case of Memb-I). For Memb-II and III the effect will slightly different because of the variation of the amino group present on the membrane. It follows the same trend in the case of other two salts.

3.2. Separation of organics

Thin film polyamide composite membranes become increasingly popular in organic separation from water. Glucose, sucrose is taken as

Table 4
Volume flux (J_v) of different salts.

J_v (LMH)			
	Memb I	Memb II	Memb III
NaCl	88.2 ± 1.80	34.11 ± 2.77	38.41 ± 1.63
Na$_2$SO$_4$	83.2 ± 0.80	33.27 ± 2.22	38.41 ± 2.06
MgSO$_4$	84.7 ± 2.77	33.17 ± 2.49	38.61 ± 1.98
MgCl$_2$	83.16 ± 1.14	34.89 ± 0.49	43.06 ± 1.27
CaCl$_2$	82.67 ± 0.57	35.64 ± 1.14	41.82 ± 1.48

molecular descriptors. Molecular weight is primarily used parameter reflecting molecular size, although it is not a direct measure of molecular size. The separation study shows that R$_{sucrose}$ > R$_{glucose}$. Fig. 11 shows the effect of pH in terms of separation performance for the membranes. At high pH condition the membranes are more negatively charged as the zeta potential value suggests and glucose in glucosate form [41].

The electrostatic repulsion between membrane and the ions increases and it leads to shrinkage of pores. It results higher retention and lower flux in alkaline pH. In acidic pH, the membranes are showing lower zeta potential because of the undissociated carboxyl groups as well as adsorption of protons [42].

Thus, the shrinkage occurs of the nodule entity of the polymeric inbuilt structure and shows enlargement of pores. It results low retention. The separation performances for three membranes are compared and follows the trend Memb-II > Memb-III > Memb-I. The acetonitrile-water (1:1) mixture of piperizine in the interfacial polymerization reaction optimizes the permeability as well as the charge factor of Memb-II.

Fig. 12 shows the variation of separation performance with pH. The trend shows that isoproturon have higher separation data with respect to diuron. These findings can be explained from the molecular size as well as polarity, ensemble in Table 1. The lower molecular size as well as relatively high polarity facilitates diuron to pass through all the
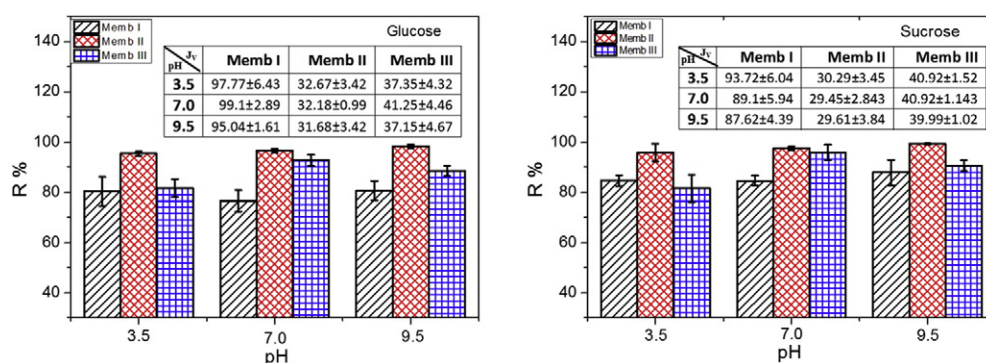
Fig. 11. Variation of separation performances of glucose and sucrose with pH.

charged membranes. Similar separation performance order for three membranes is Memb-II > Memb-III > Memb-I. The maximum rejection of diuron for our membrane (Memb-II, having 68.7% NaCl rejection) is 79.34% compared to Film tech (Dow) membrane, having 75% NaCl rejection which shows 87% rejection almost same pressure [43].

The separation performance of diuron (having relatively higher dipole moment) in higher pH decreases, as there are the possibilities to pass through the membranes having zeta potential relatively more negative. The statistical population of polar molecules near the vicinity of charged membrane increases and thus there are the chances to pass through the membranes [44]. The rejection difference is not very much reflected for Memb-I, which is more porous, reflected from its flux. The relatively low polarity of isoproturon as well as higher molecular size follows the reverse trend, i.e. at higher pH the separation increases.

In acidic pH these two urea herbicides exist as cationic species (DH$^+$) as shown [45] and the membranes show positively charged as zeta potential suggests. The repulsive interactions for higher size isoproturon may be the possible explanation for the increase in separation. But, in case of diuron may be widening of pores in acidic condition is the reason for decrement in separation.

4. Conclusions

Thin film polyamide composite membranes were prepared through interfacial polymerization varying piperizine solvent (viz. water, acetonitrile-water, acetonitrile) with trimesoyl chloride in hexane. The difference is due to the partition co-efficient of piperizine in these solvents with hexane. Though the separation of salts follows the order Memb-III to Memb-I, the selectivity of bivalent to monovalent salts (SO$_4^=$/Cl$^-$) decreases from Memb-I to Memb-III i.e. varying solvents water > acetonitrile-water > acetonitrile. The pH dependence salt separation effect is quite different for three membranes. The separation at its minimum for NaCl at pH 7, whereas it show an increasing trend in acidic as well as alkaline pH. All

three membranes show decreasing trend for Na$_2$SO$_4$ and MgSO$_4$ separation in acidic pH. Memb-III shows detrimental effect in alkaline pH may be due to counter-ion effect as well as competitive OH$^-$ effect.

The organics separation performance order for the three membranes is Memb-II > Memb-I > Memb-III. The physical properties of the feed organics also show their order (R$_{sucrose}$ > R$_{glucose}$) (R$_{isoproturon}$ > R$_{diuron}$) for the same membranes. The difference in pH effect is because of the polarity and molecular size difference along with the nature of the membranes. The isoproturon separation is in increasing trend in high and low pH where as diuron suffers a detrimental effect for Memb-II and Memb-III.

Acknowledgement

References

[1] J.E. Cadotte, R.J. Petersen, Thin-Film Composite Reverse-Osmosis Membranes, Origin, Development, and Recent Advances [Water Purification], in: ACS Symposium Series (USA), American Chemical Society, 1981.

[2] R.J. Petersen, Composite reverse osmosis and nanofiltration membranes, J. Membr. Sci. 83 (1993) 81–150.

[3] A.P. Rao, S. Joshi, J. Trivedi, C. Devmurari, V. Shah, Structure–performance correlation of polyamide thin film composite membranes: effect of coating conditions on film formation, J. Membr. Sci. 211 (2003) 13–24.

[4] W.E. Mickols, Composite membrane and method for making the same, in, (US Patent 6,337,018), 2002.

[5] J.E. Tomaschke, Amine monomers and their use in preparing interfacially synthesized membranes for reverse osmosis and nanofiltration, in, (US Patent 5,922,203), 1999.

[6] A. Ahmad, B. Ooi, Properties–performance of thin film composites membrane: study on trimesoyl chloride content and polymerization time, J. Membr. Sci. 255 (2005) 67–77.

[7] M.M. Chau, W.G. Light, X.A. Swamikannu, Chlorine-tolerant, thin-film composite membrane, in, (US Patent 5,271,843), 1993.
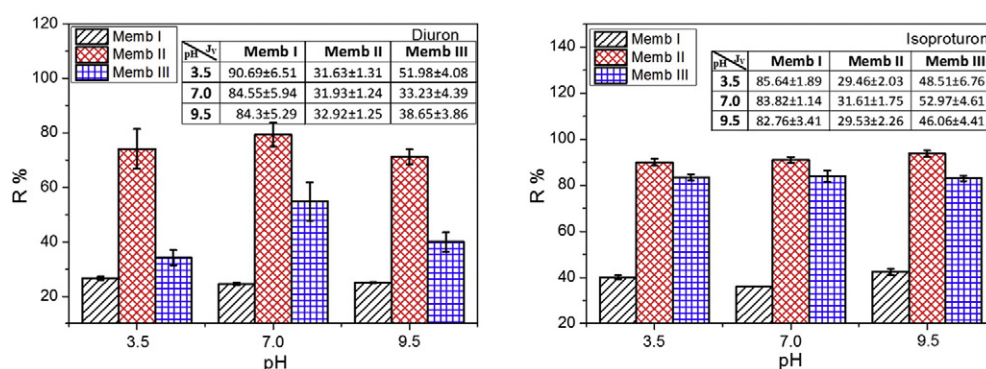
Fig. 12. Variation of separation performances of diuron and isoproturon with pH.

[8] H. Hachisuka, K. Ikeda, Reverse osmosis composite membrane and reverse osmosis treatment method for water using the same, in, (US Patent 6,413,425), 2002.

[9] S. Verissimo, K.-V. Peinemann, J. Bordado, Thin-film composite hollow fiber membranes: an optimized manufacturing method, J. Membr. Sci. 264 (2005) 48–55.

[10] S.H. Kim, S.-Y. Kwak, T. Suzuki, Positron annihilation spectroscopic evidence to demonstrate the flux-enhancement mechanism in morphology-controlled thin-film-composite (TFC) membrane, Environ. Sci. Technol. 39 (2005) 1764–1770.

[11] S.-Y. Kwak, S.G. Jung, S.H. Kim, Structure-motion-performance relationship of flux-enhanced reverse osmosis (RO) membranes composed of aromatic polyamide thin films, Environ. Sci. Technol. 35 (2001) 4334–4340.

[12] J. Jegal, S.G. Min, K.H. Lee, Factors affecting the interfacial polymerization of polyamide active layers for the formation of polyamide composite membranes, J. Appl. Polym. Sci. 86 (2002) 2781–2787.

[13] R. Lo, A. Bhattacharya, B. Ganguly, Probing the selective salt rejection behavior of thin film composite membranes: a DFT study, J. Membr. Sci. 436 (2013) 90–96.

[14] F.J. Benitez, J.L. Acero, F.J. Real, C. Garcia, Removal of phenyl-urea herbicides in ultra-pure water by ultrafiltration and nanofiltration processes, Water Res. 43 (2009) 267–276.

[15] V. Ermatchkov, Á. Pérez-Salado Kamps, D. Speyer, G. Maurer, Solubility of carbon dioxide in aqueous solutions of piperazine in the low gas loading region, J. Chem. Eng. Data 51 (2006) 1788–1796.

[16] P. Manna, H. Brahmbhatt, D. Sahu, B. Ganguly, A. Bhattacharya, On the differences of separation of hazardous catechol and resorcinol through tailor-made thin film composite (TFC) membranes, J. Environ. Chem. Eng. 3 (2015) 1758–1768.

[17] B.S. Lalia, V. Kochkodan, R. Hashaikeh, N. Hilal, A review on membrane fabrication: structure, properties and performance relationship, Desalination 326 (2013) 77–95.

[18] R. Mehta, H. Brahmbhatt, N. Saha, A. Bhattacharya, Removal of substituted phenyl urea pesticides by reverse osmosis membranes: laboratory scale study for field water application, Desalination 358 (2015) 69–75.

[19] S. Asai, S. Majumdar, A. Gupta, K. Kargupta, S. Ganguly, Dynamics and pattern formation in thermally induced phase separation of polymer–solvent system, Comput. Mater. Sci. 47 (2009) 193–205.

[20] W. Zhao, Y. Su, C. Li, Q. Shi, X. Ning, Z. Jiang, Fabrication of antifouling polyethersulfone ultrafiltration membranes using Pluronic F127 as both surface modifier and pore-forming agent, J. Membr. Sci. 318 (2008) 405–412.

[21] G. Kapantaidakis, G. Koops, M. Wessling, Effect of spinning conditions on the structure and the gas permeation properties of high flux polyethersulfone—polyimide blend hollow fibers, Desalination 144 (2002) 121–125.

[22] F. Khalili, A. Henni, A.L. East, pKa values of some piperazines at (298, 303, 313, and 323) K, J. Chem. Eng. Data 54 (2009) 2914–2917.

[23] L.G. Gagliardi, C.B. Castells, C. Rafols, M. Rosés, E. Bosch, Static dielectric constants of acetonitrile/water mixtures at different temperatures and Debye-Hückel a and a 0 B parameters for activity coefficients, J. Chem. Eng. Data 52 (2007) 1103–1107.

[24] B.J. Herbert, J.G. Dorsey, n-Octanol–water partition coefficient estimation by micellar electrokinetic capillary chromatography, Anal. Chem. 67 (1995) 744–749.

[25] M. Fontyn, K. van't Riet, B. Bijsterbosch, Surface spectroscopic studies of pristine and fouled membranes part 1. Method development and pristine membrane characterization, Colloids Surf. 54 (1991) 331–347.

[26] S. Belfer, R. Fainchtain, Y. Purinson, O. Kedem, Surface characterization by FTIR-ATR spectroscopy of polyethersulfone membranes-unmodified, modified and protein fouled, J. Membr. Sci. 172 (2000) 113–124.

[27] N. Misdan, W.J. Lau, A.F. Ismail, T. Matsuura, D. Rana, Study on the thin film composite poly (piperazine-amide) nanofiltration membrane: impacts of physicochemical properties of substrate on interfacial polymerization formation, Desalination 344 (2014) 198–205.

[28] Y. Liu, S. Zhang, Z. Zhou, J. Ren, Z. Geng, J. Luan, G. Wang, Novel sulfonated thin-film composite nanofiltration membranes with improved water flux for treatment of dye solutions, J. Membr. Sci. 394 (2012) 218–229.

[29] V.T. Do, C.Y. Tang, M. Reinhard, J.O. Leckie, Degradation of polyamide nanofiltration and reverse osmosis membranes by hypochlorite, Environ. Sci. Technol. 46 (2012) 852–859.

[30] M. Ionita, A.M. Pandele, L.E. Crica, A.C. Obreja, Preparation and characterization of polysulfone/ammonia-functionalized graphene oxide composite membrane material, High Perfor. Polym. 1-8 (2015).

[31] A. Bhattacharya, P. Ghosh, Nanofiltration and reverse osmosis membranes: theory and application in separation of electrolytes, Rev. Chem. Eng. 20 (2004) 111–173.

[32] V. Freger, Nanoscale heterogeneity of polyamide membranes formed by interfacial polymerization, Langmuir 19 (2003) 4791–4797.

[33] C. Bartels, R. Franks, S. Rybar, M. Schierach, M. Wilf, The effect of feed ionic strength on salt passage through reverse osmosis membranes, Desalination 184 (2005) 185–195.

[34] J. Peeters, J. Boom, M. Mulder, H. Strathmann, Retention measurements of nanofiltration membranes with electrolyte solutions, J. Membr. Sci. 145 (1998) 199–209.

[35] W. Deen, Hindered transport of large molecules in liquid-filled pores, AICHE J. 33 (1987) 1409–1425.

[36] A. Ahmad, B. Ooi, A.W. Mohammad, J. Choudhury, Composite nanofiltration polyamide membrane: a study on the diamine ratio and its performance evaluation, Ind. Eng. Chem. Res. 43 (2004) 8074–8082.

[37] W.R. Bowen, A.W. Mohammad, N. Hilal, Characterisation of nanofiltration membranes for predictive purposes—use of salts, uncharged solutes and atomic force microscopy, J. Membr. Sci. 126 (1997) 91–105.

[38] C. Labbez, P. Fievet, A. Szymczyk, A. Vidonne, A. Foissy, J. Pagetti, Retention of mineral salts by a polyamide nanofiltration membrane, Sep. Purif. Technol. 30 (2003) 47–55.

[39] J. Schaep, C. Vandecasteele, A.W. Mohammad, W.R. Bowen, Modelling the retention of ionic components for different nanofiltration membranes, Sep. Purif. Technol. 22 (2001) 169–179.

[40] X.-L. Wang, T. Tsuru, M. Togoh, S.-i. Nakao, S. Kimura, Evaluation of pore structure and electrical properties of nanofiltration membranes, J. Chem. Eng. Jpn 28 (1995) 186–192.

[41] G. Kilde, W. Wynne-Jones, The mutarotation and electrolytic dissociation of glucose in alkaline solution, Trans. Faraday Soc. 49 (1953) 243–251.

[42] M. Ernst, A. Bismarck, J. Springer, M. Jekel, Zeta-potential and rejection rates of a polyethersulfone nanofiltration membrane in single salt solutions, J. Membr. Sci. 165 (2000) 251–259.

[43] I. Musbah, D. Cicéron, A. Saboni, S. Alexandrova, Retention of pesticides and metabolites by nanofiltration by effects of size and dipole moment, Desalination 313 (2013) 51–56.

[44] A. Bhattacharya, Remediation of pesticide-polluted waters through membranes, Sep. Purif. Rev. 35 (2006) 1–38.

[45] M. Fontecha-Cámara, M. López-Ramón, M. Alvarez-Merino, C. Moreno-Castilla, Effect of surface chemistry, solution pH, and ionic strength on the removal of herbicides diuron and amitrole from water by an activated carbon fiber, Langmuir 23 (2007) 1242–1247.